Dynamic of Launch Vehicle with Slosh Effects CILAMCE-PANACM-2021

Domingos Sávio Aguiar[1], Carlos d'Andrade Souto[1]

[1]*Dept. of Science and Aerospace Technology – Institute of Aeronautics and Space – ACE / AIE Divisions 12228-904, São Paulo, São José dos Campos, Brasil.*
domingosdsa@fab.mil.br, *soutocds@fab.mil.br*

Abstract. The use of liquid propelled rocket engines in launcher vehicles offers many advantages over its solid counterparts: higher specific impulse; the possibility of re ignition and the control of thrust vector magnitude. The launch vehicle experiences different dynamics environments during its mission, which can affect the propellant tanks and drive oscillations of the liquid volume center of mass. Since the mass of liquid propellants in a launcher can be significant in relation to the whole vehicle mass, oscillations in the fluid volumes can lead to important dynamic effects. In this work, the dynamics characteristics of a launch vehicle with liquid propellant are analyzed considering lateral slosh effects. The launch vehicle body is modelled as a beam and the liquid is modelled by a spring-mass system. The natural frequencies and mode shapes of the vehicle with and without including the liquid sloshing modes are evaluated for different fill ratios of the propellant tanks.

Keywords: Launch vehicle; slosh, finite element method (FEM), mode shapes, natural frequency.

1 Introduction

The use of liquid propelled rocket engines in launcher vehicles offers many advantages over its solid counterparts: higher specific impulse; the possibility of re ignition and the control of thrust vector magnitude, Sutton [1]. Thus, during the evolution of commercial launch service, liquid-powered vehicles dominate this scene due to these specific characteristics as can be observed in, Schlingloff [2].

The motion of liquids in partially filled tanks is known as the sloshing effect. Strong coupling between the sloshing effect, the mechanical structure and the control system can occur. It is then rather important to account for this effect in a launcher, Rossi et al. [3]. A practical way to analysis slosh effects on launcher vehicle consists of replacing the liquid conceptually by an equivalent linear mechanical system, and thus including the dynamic effects of sloshing in the launcher dynamic model, Barrows and Orr [4]. Several methods have been developed to describe propellant sloshing modes and frequencies. It can be shown for a cylindrical tank that spring-mass analogies can be devised which will reproduce the characteristics of the mode of sloshing oscillation, Schuett et al. [5].

A launcher vehicle is a very long flexible structure. The general approach for dynamic solutions involving large systems is to develop a mathematical model describing the system's mass and stiffness to calculate natural frequencies and mode shapes of vibration. AGARD-115 [6].

The structural dynamic models in form of mass and stiffness are usually constructed from finite element method (FEM), which may also contain the liquid propellant of the tanks, NASA-HDBK-7005 [7]. Part of this propellant can be considered as rigid or distributed mass on the idealized beam while a smaller portion must be allowed to sloshing in the lateral model, which is described in details by Ibrahim [8], Dodge [9] and Abramson [10].

In this paper, the structural dynamic behavior of a launch vehicle with two liquid propellant stages is evaluated. The natural frequencies and mode shapes of the vehicle with and without including the liquid sloshing modes are evaluated for different fill ratios of the propellant tanks during first stage flight.

2 Mechanical Slosh Model

In the present study, the lateral slosh model for a cylindrical tank partially filled liquid propellant, Fig. 1, based on a set of spring-masses. The geometry of the cylindrical tank consists of its height, *H*, and diameter, *d*. Its volume depends on fill of the tank when the actual liquid level is equal to *h*.

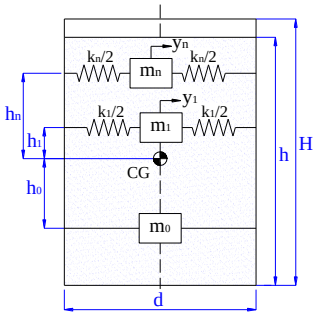

Figure 1. Spring-mass slosh model for cylindrical tank.

According to Abramson [10], the action of lateral sloshing, represented by a set of spring-mass systems, it causes the displacement, y_n, of slosh mass, m_n , with respect to the tank wall. Each of the spring constant, k_n is chosen such their ratio to the oscillating mass is equal to the square of natural frequency, ω_n^2 , of that mode; that is:

$$\omega_n^2 = \frac{k_n}{m_n} = \frac{2\xi_n g}{d}\ tanh\left(\frac{\xi_n h}{d}\right) \tag{1}$$

where the parameters m_n and k_n are given by:

$$m_n = m_{liq}\left[\frac{d}{h\left(\xi_n^2 - 1\right)}\right] tanh 2\xi_n \frac{h}{d} \tag{2}$$

$$k_n = m_{liq}\left[\frac{2g}{h\left(\xi_n^2 - 1\right)}\right]\left[tanh 2\xi_n \frac{h}{d}\right]^2 \tag{3}$$

In the above equations m_{liq} is mass of the liquid and ξ_n are the roots of specific Bessel functions. The slosh mass, m_n, has a distance with respect to the center of gravity of the tank of:

$$h_n = \frac{h}{2} - \frac{d}{\xi_n}\ tanh\left(\frac{\xi_n h}{d}\right) \tag{4}$$

The mass m_0 is a static mass, i.e., that portion of the liquid that does not move and h_o its location with respect to the center of gravity of the tank respectively given by:

$$m_0 = m_{liq} - \sum_{i=1}^{n} m_n \tag{5}$$

$$h_0 = \frac{1}{m_0}\sum_{i=1}^{n} m_s h_n \tag{6}$$

The total mass of the liquid, m_{liq} , is a function on the fill ratio of the tank, and the liquid density, ρ_{liq}.

$$m_{liq} = \frac{\pi}{4} d^2 h\, \rho_{liq} \tag{7}$$

3 Structural Dynamic Model

3.1 Natural frequencies and mode shapes

Since nonlinearities are not accounted for in the model, the motion of complete system is represented by:

$$[M]\{\ddot{u}\}+[C]\{\dot{u}\}+[K]\{u\}=\{f\} \tag{8}$$

where, $[M]$, $[C]$ and $[K]$ are, respectively, mass, damping and stiffness matrices. Displacements, velocities and accelerations are represented by $\{u\}$, $\{\dot{u}\}$ and $\{\ddot{u}\}$, respectively. On the right hand side, $\{f\}$ represents the forces acting on the system. In order to perform a modal analysis of the structural system represented by eq. (8), the damping and externally applied forces are neglected:

$$[M]\{\ddot{u}\}+[K]\{u\}=\{0\} \tag{9}$$

Thus, if one writes the displacement in the form:

$$\{u(y,t)\}=\{\phi(y)\}\sin\Omega(t-t_o) \tag{10}$$

where ϕ is a vector of order n, t the time variable, t_o a time constant, and Ω a constant identified to represent the frequency of vibration of the vector ϕ, substituting eq. (10) into eq. (9) results the generalized eigenproblem:

$$\left[[K]+\Omega^2[M]\right]\{\phi\}=\{0\} \tag{11}$$

from which ϕ, the mode shape and Ω, natural frequencies can be determined, Craig and Kurdila [11].

3.2 Launch vehicle model

The Figure 2 shows the layout of a conceptual launch vehicle whose data are available in Zhuang and Yulin [12]. Its length L is 16.2 m and diameter D of 1.0 m with payload capacity of 100 kg and both stages use LOX/RP-1 as propellant. The structural parts such as aft stage, tanks and inter-stage with thickness of 5 mm use Al alloy: Young's modulus 72.4 GPa, Poisson's ratio 0.31 and density 2780 kg/m^3. The fairing with thickness of 3 mm uses composite material with equivalent properties: Young's modulus 240 GPa, Poisson's ratio 0.33 and density of 1594 kg/m^3. The masses of the propulsive subsystems and electronics components related to the first and second stages are 130 and 135 kg, respectively and its adapter cone with electronics has 52 kg. The density of oxidiser and fuel are 1140 and 820 kg/m^3, respectively.

Finite Element package FEMAP Nx Nastran [13] was used to model and analysis the dynamic structure of the launch vehicle. Due to large (L/D) ratio the beam model is adequate for capturing the flexibility effects. The propellant can be considered as rigid or distributed mass on the idealized beam while a smaller portion must be allowed to sloshing in the lateral model. Basically, beam elements, lumped mass element and linear spring elements were used, Fig. 2. The launch vehicle model contain a total of 172 elements.

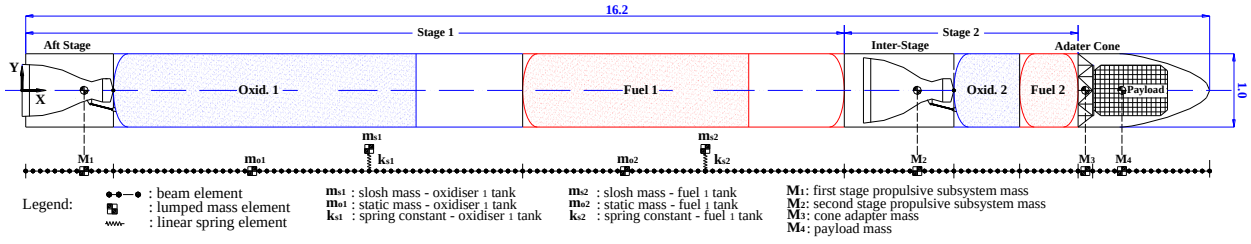

Figure 2. Launch vehicle layout and finite element model.

4 Results

4.1 Slosh parameters

First of all, in order to analyze the dynamic of the launch vehicle with slosh effects considering the first stage flight, the calculations of the slosh parameters were performed, eqs. (1) up to (7). The data related to a burn time of the 151s and thrust of 165 kN, present in Zhuang and Yulin [12], were used to establish fill ratio (FR) and the *g* value adjusts. The fill ratio is linearly decreasing with burn time and the volume due to mass depletion is considered proportional in both tanks. The *g* values were adjusted due to axial acceleration of the vehicle taking into account an adopted curve thrust as well as the change of the vehicle mass. The higher modes are neglected due to very small slosh mass involved, Abramson [10]. Therefore, only the first mode is considered and in this case the root of specific Bessel functions is ξ_1=1.841, Abramson [10]. The Table 1 presents the slosh parameters values for oxidiser-1 and fuel-1 tanks considering the fill ratios of 75%, 50% and 25%, respectively.

Table 1. Slosh parameters

Oxidiser-1 tank.									
m_s (kg)	k_s (N/m)	h_s (m)	*f_s (Hz)	m_o (kg)	h_o (m)	h (m)	cg (m)	FR	m_{liq} (kg)
203.55	13851.53	1.53	1.3129	3503.97	0.09	4.141	2.070	75%	3707.52
203.55	10419.97	0.83	1.1387	2257.19	0.07	2.748	1.374	50%	2460.74
203.53	8349.54	0.14	1.0194	1010.43	0.03	1.356	0.678	25%	1213.97
Fuel-1 tank.									
m_s (kg)	k_s (N/m)	h_s (m)	*f_s (Hz)	m_o (kg)	h_o (m)	h (m)	cg (m)	FR	m_{liq} (kg)
146.41	9963.38	1.00	1.3129	1845.66	0.080	3.093	1.547	75%	1992.07
146.41	7495.05	0.48	1.1387	1175.76	0.060	2.053	1.026	50%	1322.17
146.25	5993.08	0.01	1.0188	506.03	0.003	1.013	0.506	25%	652.27

* $f_s=\omega_s/2\pi$

4.2 Launch vehicle natural frequencies and mode shapes

Natural frequencies and mode shapes of the launch vehicle with slosh effects were calculated considering the parameters presents in Tab.1. The mode shapes are presented together with the undeformed shape in plane XY, according to the coordinate system of the vehicle, displayed in Fig. 2. The results showed that the dynamic characteristics of the vehicle present either vibratory behavior with predominant slosh frequency f_s or structural bending frequencies f_b with respect to fill ratios evaluated. Some remarks related to respective vibratory behavior are described as following:

Slosh frequencies and mode shapes: Firstly, the data in the Tab. 1 show that slosh frequencies either oxidiser-1 tank or fuel-1 tank practically present the same values with respect to fill ratios. The mode shapes of the vehicle that correspond to the frequencies (rigid body modes) are present in Fig. 3. Its frequencies are very close to these presented in Tab. 1. About vehicle values mode shapes, there are two different modes associated to sloshing. In lower frequency mode (a) the slosh masses oscillate out of phase, the greatest amplitudes of displacement of the vehicle appear in the forward region and increase more and more as the fill ratio decreases. In the higher frequency mode (b) the slosh masses oscillate in phase, the greatest amplitudes of displacement of the vehicle appear in the aft region and increase more and more as the fill ratio decreases.

Bending frequencies and mode shapes: The Figure 4 presents the vehicle mode shapes related to bending frequencies with slosh masses effects. The analysis takes into account only the first and second modes with respect to fill ratios evaluated. In this case, the slosh masses tend to remain around their equilibrium position in relation to the displacement amplitudes of the modal forms. There is a tendency for the frequency to increase as the fill ratio decreases. Finally, simulations were performed without the slosh mass effect, and the frequency values were compared with the data presented in Fig. 4. The results are displayed in Tab. 2, and show that the frequency values are very close. The remarks presented here should be also assumed for modes and frequencies with superior orders.

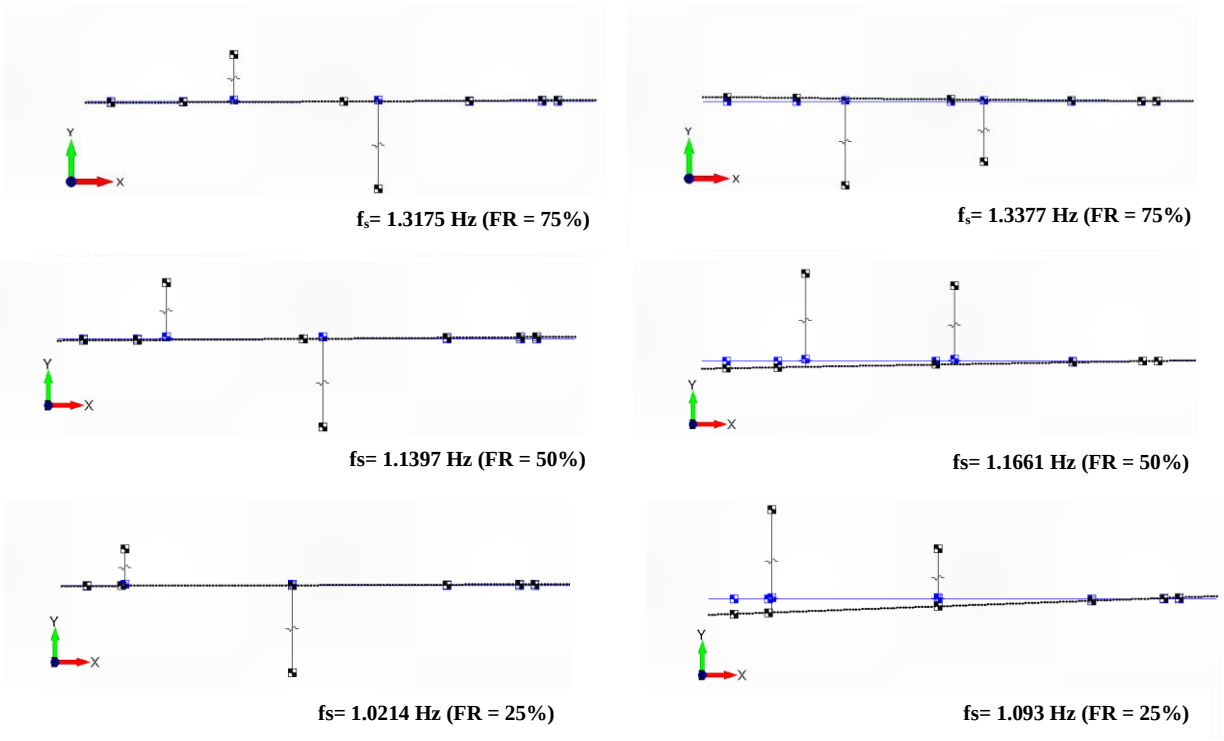

Figure 3. Natural frequency and mode shape in XY plane: (a) first slosh mode and (b) second slosh mode

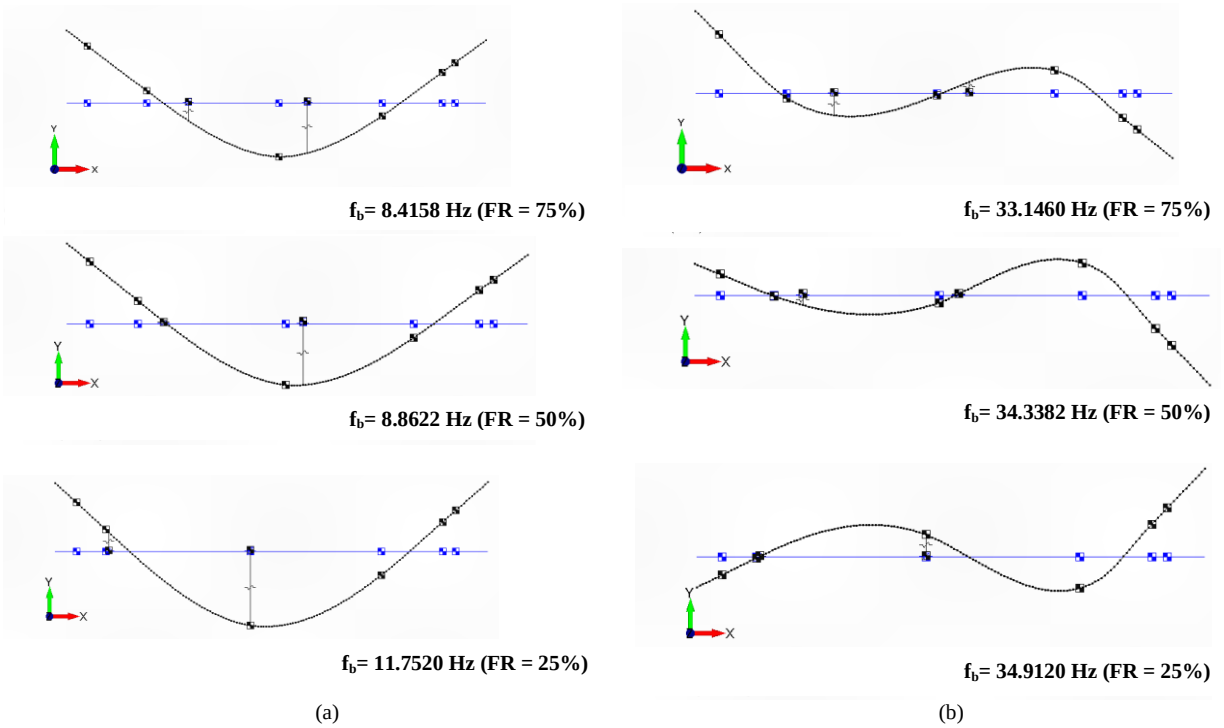

Figure 4. Natural frequency and mode shape in XY plane: (a) first bending mode and (b) second bending mode

Table 2. First and second bending modes frequencies with and without slosh masses

Mode 1				Mode 2			
FR	f_1 (Hz)	f_2 (Hz)	Δf	FR	f_1 (Hz)	f_2 (Hz)	Δf
75%	8.4158	8.4118	0.047%	75%	33.1460	34.1456	0.001%
50%	8.8622	8.6164	0.060%	50%	34.3382	34.8199	0.005%
25%	11.7520	11.6262	1.071%	25%	34.9120	34.0712	2.408%

f_1: frequencies with slosh mass
f_2: frequencies without slosh mass

5 Conclusions

A conceptual launch vehicle with two liquid propellant tanks was used to evaluate its structural dynamic with slosh effects during first stage flight. Natural frequencies and vehicle structural mode shapes were calculated with fill ratios of 75%, 50% and 25% by finite element analysis. The results show that slosh frequencies of vehicle are like these calculated for both tanks by theory presented in Abramson [10], which shows the capability of a simplified finite element model to reproduce slosh effects in launcher structure. The presence of slosh masses little changed the first 2 natural frequencies of the structure (two bending modes). This was possibly caused by the small slosh masses (compared to the total vehicle mass) involved which in turn is due to the geometry of the tanks (high length/diameter ratio). A natural continuation of this work is to use the same methodology to verify the influence of slosh masses on the natural frequencies of the structure of a launcher with vertical cylindrical tanks with different length/diameter ratios than the vehicle analyzed here.

Acknowledgements. The authors thank CAPES for the PROAP grant for the publication of this article and the IAE for its support in carrying out this work.

Authorship statement. The authors hereby confirm that they are sole liable persons responsible for the authorship of this work, and that all material that has been herein included as part of the present paper is either the property (and authorship) of authors or has the permission of the owners to be included here.

References

[1] G.P. Sulton, “History of Liquid Propellant Rocket Engine”. Virginia: AIAA, 2006.
[2] H.Schlingloff, “Astronautical Engineering – An introduction to the Technology of Spaceflight” Bad Abbach, Germany 2005.
[3] V. Rossi, S.Schäff, S.ven Weiker, A.Wiegand. “Multibody Feature for Simulation of Flexible Launcher Dynamics”. Astos 9.3. Astos Solutions GmbH, Stuttgart (Germany)
[4] T. Barrows and J. Orr. “Dynamic and Simulation of Flexible Rockets”, Elsevier Inc. 2021.
[5] R.H.Schuett, B.A. Appleby and J. D. Martin, “Dynamic Loads Analysis of Space Vehicle Systems-Launch and Exit Phase;” NASA, 1966.
[6] AGARD-115, “Wind Effects on Launch Vehicles”. The Advisory Group for Aerospace Research and Development, NATO, England, 1970.
[7] NASA-HDBK -7005 - ,” Dynamic Environmental Criteria” NASA Technical Handbook, March,2001.
[8] R.A.Ibrahim, “Liquid Sloshing Dynamics – Theory and Applications” – Cambridge, 2005.
[9] F. Dodge, “The New Dynamic Behavior of Liquids in Moving Containers,” Southwest Research Institute, 2000.
[10] Abramson, H.N., “The dynamic behavior of liquids in moving containers: with applications to space vehicle technology",
NASA SP-106, 1966.
[11] R.R. Craig,Jr and A.J. Kurdila. “ Fundamentals of Structural Dynamics”. John Wiley and Sons- Second Edition 2006.
[12] L. Zhuang and Z. Yulin, “Deformation Reconstruction and High-Precision Attitude Control of a Launch Vehicle Based on Strain Measurements.” International Journal of Aerospace Engineering – Hindawi. February, 2021.
[13] FEMAP Nx Nastran – Educational License, 2014.